

Rational Design and Binding of Modified Cell-Wall Peptides to Vancomycin-Group Antibiotics: Factorising Free Energy Contributions to Bindings[§]

Stephen E. Holroyd, Patrick Groves, Mark S. Searle, Ute Gerhard and
Dudley H. Williams*

Cambridge Centre for Molecular Recognition
University Chemical Laboratories, Lensfield Road, Cambridge CB2 1EW, UK.

(Received in USA 2 February 1993; accepted 26 March 1993)

Abstract: Modified cell-wall peptides have been rationally designed and studied in a semi-quantitative approach to factorising free energy contributions in binding to vancomycin-group antibiotics in aqueous solution. Binding energies for succinyl and fumaryl-D-Ala dipeptides, and N-oxalyl- γ -aminobutyric acid analogues, are compared with binding energies for the natural substrate N-Ac-D-Ala-D-Ala, and the truncated mono-peptide N-Ac-D-Ala. We estimate the binding energy of the N-terminal carboxyl group, by four independent analyses, to be $-(14 \text{ to } 17) \pm 7 \text{ kJ mol}^{-1}$ when differences in ligand binding energies are corrected for differences in contributions from the "cost" of restricting rotations and "benefits" of hydrophobic interactions. The carboxylate interaction comprises both a charged $-\text{COO}^-\cdots\text{HN}^+$ hydrogen bond plus face to face π -stacking between the carboxylate group and an aromatic ring in the antibiotic binding pocket.

INTRODUCTION

Vancomycin-group antibiotics bind small peptide fragments of the cell-wall peptidoglycan of gram-positive bacteria, providing a paradigm for quantitative studies of molecular recognition phenomena *in vitro*. In several recent papers,¹⁻³ building upon the principles outlined in the classic work by Page & Jencks,^{4,5} we have presented a factorisation of free energy contributions to binding through studies of peptide analogues and fragments of the key recognition sequence N-Ac-D-Ala-D-Ala. In the general case, the binding "benefits" and "costs" are considered as the sum of the six terms collected together in equation (1):

$$\Delta G = \Delta G_{T+R} + \Delta G_r + \Delta G_h + \sum \Delta G_p + \Delta G_{\text{conf}} + \Delta G_{\text{vdw}} \quad (1)$$

Using the method of ligand extension or modification ("anchor principle"),⁴ we have compared the binding of ligand X-Y-Z and ligand X-Y in which the ΔG_{T+R} term (the cost of a bimolecular association, involving the loss of translational and rotational entropy) can usefully be regarded as common to both associations, and is thereby a variable which is removed from the equation.⁶ Thus, the difference in binding energy ($\Delta\Delta G$) between X-Y-Z and X-Y can be attributed to the functional group contributions of Z after allowance has been made for any additional free energy costs associated with additional rotors restricted ($\Delta\Delta G_r$) in the bonds connecting Y and Z, and for any additional hydrophobic effects ($\Delta\Delta G_h$) expressed by the addition of Z. The side chains of the

[§] Submitted in honour of Carl Djerassi on the occasion of his 70th birthday.

antibiotic are cross-linked, and hence, to a useful approximation, its internal rotations are restricted both before and after binding. Where very small structural changes are compared, or where truncated ligands are considered in which associations occur without any significant difference in conformational strain ($\Delta\Delta G_{\text{conf}} \approx 0$; bound conformations are close to the energy minima of the free ligand), and where no cavities and/or van der Waals repulsions are introduced ($\Delta\Delta G_{\text{vdW}} \approx 0$), a more practical form of equation (1), and one that is more readily applied experimentally is:

$$\Delta\Delta G = \Delta\Delta G_r + \Delta\Delta G_h + \Delta(\Sigma\Delta G_p) \quad (2)$$

Here $\Delta\Delta G_h$ corresponds to the difference in free energy contribution from the hydrophobic effect (a property of binding in aqueous solution, arising from the removal of hydrocarbon from exposure to solvent). $\Sigma\Delta G_p$ is the sum of the free energy contributions from the polar group interactions and any other favourable electrostatic interactions introduced by the Z binding component.

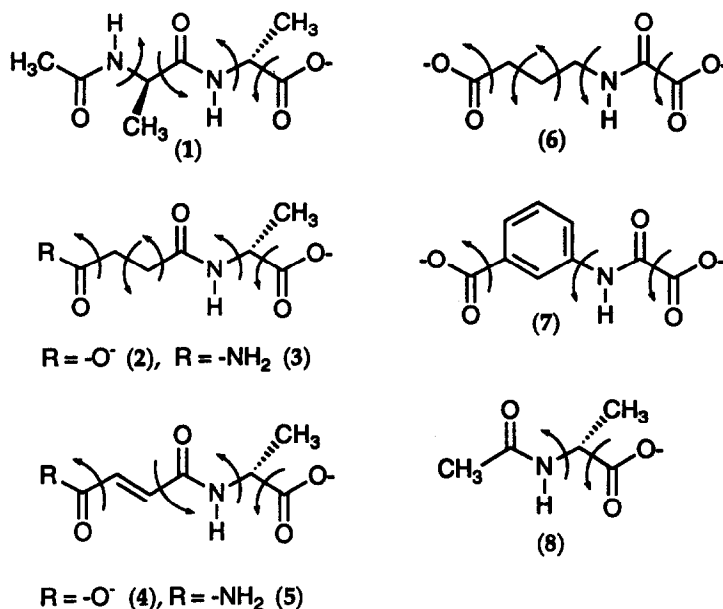


Figure 1: Ligand structures 1–8. Arrows represent internal rotations restricted on binding. Methyl groups have small barriers to rotation and are unrestricted in both free and bound ligands, while peptide bonds have large barriers to rotation and are considered to be restricted both before and after binding.

In the following, we describe the rational design of ligands to probe binding contributions in solution from each of the three terms in equation (2). In Figure 1, ligands 2 to 5 represent peptide analogues of the natural substrate N-Ac-D-Ala-D-Ala (1), where the introduction of the double bond in 4 versus 2 has already enable us to assess the cost of restricting a rotation in binding to ristocetin A.⁷ Peptide ligands 3 (vs 2) and 5 (vs 4) now allow us to evaluate the relative contribution of the amide-amide interaction versus the amide-carboxylate interaction. In order to give more variation in the types of ligand that can be studied, the carbonyl group from the N-terminal D-

Ala of **1** has been transposed to give the oxamic acid derivatives **6** and **7**, in which all essential functional group interactions with the antibiotic binding pocket are retained, as illustrated in Figure 2 for (A) the natural substrate (**1**), and (B) the general case.

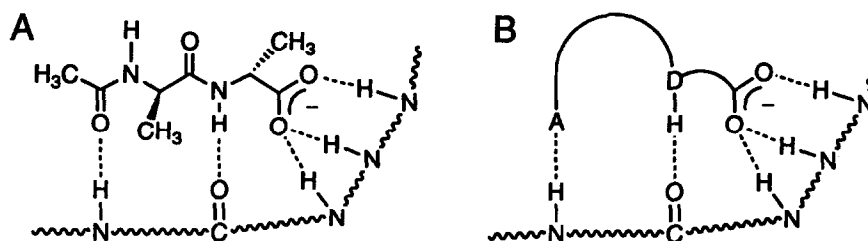


Figure 2: Intermolecular hydrogen bonds between ligands and the binding pocket of vancomycin-group antibiotics; (A) N-Ac-D-Ala-D-Ala (**1**), and (B) the general case. Serrated lines represent more than one intervening covalent bond of the antibiotic, curved lines several intervening bonds in the ligand; A and D represent hydrogen bond acceptors and donors respectively.

The transposed carbonyl groups of **6** and **7** are positioned on the solvent-exposed face of the ligand binding cavity and are not directly involved in binding. Thus, the difference in binding energy ($\Delta\Delta G$) between **6** and **7** will reflect different contributions from the hydrophobic effect between the saturated alkyl chain of **6** and the phenyl ring of **7**, and also the additional cost in free energy of restricting two extra rotors in binding **6**. On the basis of experimental data, we have previously estimated the non-polar surface area-dependence of the hydrophobic effect,² and are able to separate the contributions to the difference in binding energy between **6** and **7**, permitting an estimate of the "cost" of restricting a rotor on binding that is consistent with our earlier conclusions.^{7,12} The remaining variable in equation (2) corresponds to the *apparent* binding energy of polar functional group interactions (ΔG_p), in particular that of the N-terminal carboxylate group of ligands **2** and **6**, and the corresponding amide group of **3**. ΔG_p values estimated from the difference in binding energy with respect to the natural substrate **1** and the truncated analogue **8**, give consistently similar ΔG_p values for the carboxylate binding energy in four different ligand extension/modification comparisons.

In using this approach, we recognise that the derived ΔG_p values will be subject to varying degrees of uncertainty (as a consequence of both the approximations used in the analysis, and from experimental errors); additionally ΔG_p values may vary from one environment to another, and be further complicated by cooperativity. Nevertheless, it seems worthwhile to attempt a semi-quantitative description of binding, if only to give estimates of the parameters involved.

STRUCTURAL STUDIES BY NMR AND MOLECULAR MODELLING

An important first step is to establish structural details of the interactions of **2–7** with the antibiotics that can be directly correlated with the differences in binding energies described below. Detailed NMR studies of ligand binding will be published elsewhere. For example, intermolecular NOE data on the complex of **6** with ristocetin A (Figure 3) are consistent with the methylene protons on the γ -aminobutyric acid side chain of **6** binding to the hydrophobic pocket occupied by the N-terminal alanine methyl group of the natural substrate (**1**).⁸

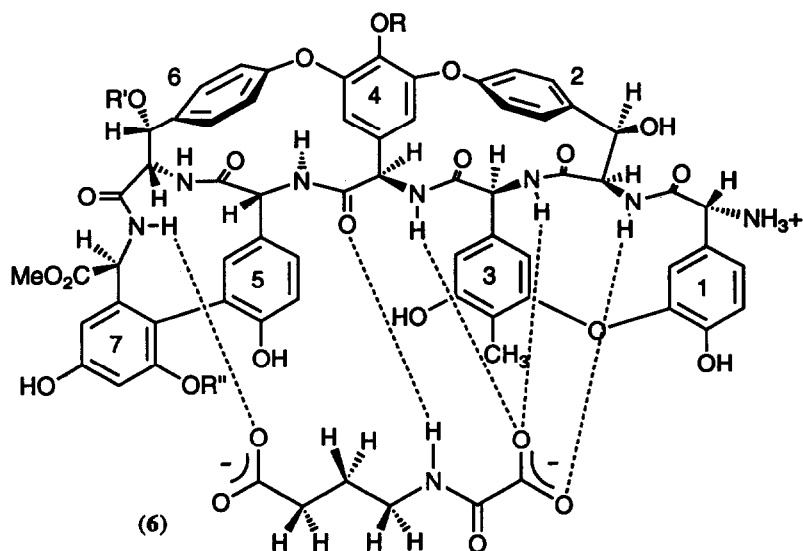


Figure 3: Complex of ligand 6 with ristocetin A. Dotted lines represent hydrogen bonds.

These NOEs can only be rationalised in terms of a binding conformation and orientation in which the butyryl carboxylate group of 6 is hydrogen bonded to the amide NH of residue 7, in an analogous manner to the N-acetyl carbonyl amide-amide interaction of the natural substrate (see Figure 2), with the oxalate anion located in the carboxylate binding pocket of 1 (Figure 3). NOE data and chemical shift perturbations monitored in complexes of ligands 2-7 are consistent with analogous binding interactions identified for 1.

Table 1: Non-polar surface area buried from solvent accessibility $\Delta\Delta A_{np}$ (\AA^2) relative to the natural substrate 1, and free energies (ΔG , kJ mol^{-1}) for binding to ristocetin A.

ligand	$-\Delta\Delta A_{np}$	ΔG
1	-	-28.8 ± 0.4 ^a
2	80	-22.5 ± 0.3 ^b
3	80	-20.3 ± 0.5 ^c
4	79	-27.9 ± 0.3 ^b
5	79	-24.0 ± 0.4 ^c
6	108	-17.7 ± 0.5 ^d
7	137	-21.5 ± 1.0 ^d
8	85	-17.4 ± 0.5 ^a

^a Rodriguez-Tebar *et al.*¹¹ (298 K); ^b Gerhard *et al.*⁷ (298 K); ^c 298 K; ^d 303 K.

For example, the Ala methyl resonance of ligands 2–5 shifts upfield by ca 0.8 ppm on binding, as does that of 1, consistent with ring-current shifts associated with the methyl group in each case binding against the face of the same aromatic ring, that of residue 4 (see Figure 3). Energy minimised structures of these complexes generated using MacroModel,⁹ and guided by NOE data, indicate good ligand-receptor van der Waals complementarity, and binding geometries that lead to average hydrogen bond lengths that are comparable (± 0.2 Å) for all of the ligands considered. In order to assess the relative contributions to binding from the hydrophobic effect, the water-accessible non-polar surface area buried was estimated from energy minimised structures (antibiotic, ligand and complex) by rolling a water molecule of radius 1.4 Å over the surface using a high density of points on a sphere within MacroModel. Estimated values for the difference in solvent-accessible non-polar surface area buried ($\Delta\Delta A_{np}$) relative to the natural substrate (1) are presented in Table 1, together with experimental ligand binding energies.

In earlier studies² we have established a useful relationship between $\Delta\Delta A_{np}$ and ΔG_b from a consideration of Ala \rightarrow Gly "mutations" (methyl group deletions) in the binding of analogues of 1, where each Å² of hydrocarbon surface buried realises -0.2 ± 0.05 kJ mol⁻¹ in binding energy, in good agreement with conclusions from protein engineering experiments (-0.23 kJ mol⁻¹).¹⁰ Subsequent estimates of the hydrophobic contribution to ligand binding energies utilise this surface-area dependence.

PARTITIONING FREE ENERGY CONTRIBUTIONS

Rotor restrictions.

The cost of restricting a rotation has been assessed from the comparison of the binding energies of 2 and 4, and has been described previously to lie in the range 3.7 ± 0.9 kJ mol⁻¹.⁷ The difference in binding energy between 2 and 4 of -5.4 kJ mol⁻¹ is concluded to arise from the restriction of approximately 1.5 bonds on account of increased double-bond character in other conjugated bonds. Estimates of changes in hydrophobic surface area buried on binding reveal no contribution from $\Delta\Delta G_b$ (i.e. $\Delta\Delta A_{np} \approx 0$, Table 1). Therefore, applying analogous arguments for the difference in binding energy between 3 and 5, the cost of a rotor restriction is derived as $3.7/1.5 = 2.5$ kJ mol⁻¹. In the general case, we have considered rotor restrictions to be adverse to binding in the range 2.0 to 4.0 kJ mol⁻¹ on the basis of the above data, and also of entropy changes in the fusion of n-alkane chains.¹² Severe restrictions evident in covalent transformations, where there is little residual torsional motion in the restricted rotor,^{5,12} may be adverse by 5 to 6 kJ mol⁻¹.

Polar group interactions—succinyl and fumaryl analogues.

Using the method of ligand extension outlined earlier, we estimate the intrinsic binding contribution from the carboxylate group of 2 by partitioning free energy contributions with respect to both 1 and the truncated analogue N-Ac-D-Ala (8), for which detailed calorimetry data has been published.¹¹ An earlier analysis² (comparing 1 with 8) has lead us to conclude that the amide-amide hydrogen bond of the acetyl group of 1 (see Figure 2) contributes -2.9 ± 1.5 kJ mol⁻¹ to binding, when allowance has been made for the restriction of two additional rotors and the burial of an extra 85 Å² of non-polar surface area in the dipeptide. We present a similar analysis of the binding of 1 versus 2. Molecular modelling on energy minimised structures indicate that the binding of 1 buries 80 Å² more hydrocarbon from solvent, restricts one fewer backbone rotation on binding but forms an amide-amide hydrogen bond with the antibiotic (NH of residue 7) versus a carboxylate interaction

Table 2: Partitioning free energy contributions in the binding of **2** and **6** versus N-Ac-D-Ala-D-Ala (**1**) and N-Ac-D-Ala (**8**) to ristocetin A in aqueous solution.

ligands	$\Delta\Delta G$	$\Delta\Delta A_{np}$	$\Delta\Delta G_h$	$\Delta\Delta G_r$	ΔG_p^a	ΔG_p^b
2 vs 1	6.3±0.7	-80	16±4	3±1	-2.9±1.5	-16±7
2 vs 8	-5.1±0.8	-5	1±0.5	9±3	-	-15±4
6 vs 1	11.1±0.9	-108	22±5	3±1	-2.9±1.5	-17±8
6 vs 8	-0.3±1.0	-23	5±1	9±3	-	-14±5

^a Binding energy of the N-acetyl amide-amide hydrogen bond of **1** deduced from ligand extension studies² (**1 vs 8**); ^b carboxylate binding energy of **2** and **6** (amide-carboxylate hydrogen bond and any other associated interactions).

with the same NH. Using the previously derived² solvent accessible surface area dependence of the hydrophobic effect of $-0.2\pm 0.05 \text{ kJ mol}^{-1} \text{ \AA}^{-2}$, together with equation (2), we estimate the binding contribution of the carboxylate group of **2** (ΔG_p):

$$(6.3\pm 0.7) = (3\pm 1) + (16\pm 4) + (2.9\pm 1.5) + \Delta G_p$$

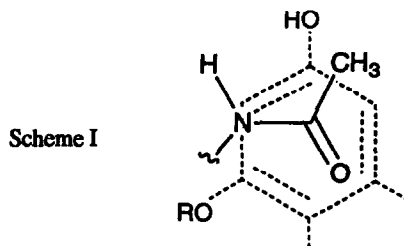
The value deduced is $\underline{ca} -16\pm 7 \text{ kJ mol}^{-1}$. A similar comparison of **2** with N-Ac-D-Ala (**8**), where the latter buries only $\Delta\Delta A_{np} = 5 \text{ \AA}^2$ more hydrocarbon surface, but where three additional rotors are restricted in the binding of **2**, and where ΔG_p again represents the binding contribution from the carboxylate group, gives:

$$-(5.1\pm 0.8) = (1\pm 0.5) + (9\pm 3) + \Delta G_p$$

Here, ΔG_p contributes $\underline{ca} -15\pm 4 \text{ kJ mol}^{-1}$ in binding energy, indicating good consistency between the two comparisons. The various contributions for these and other comparisons are summarised in Table 2.

The comparison of the binding energy of **2** versus **3**, and **4** versus **5**, indicates that the $-\text{CONH}_2$ group contributes between 2.3 ± 0.9 and $3.9\pm 0.7 \text{ kJ mol}^{-1}$ less in binding energy than the $-\text{COO}^-$ group, i.e. the former, when added as an extension on a chain of two methylene groups, has an apparent binding contribution of $\underline{ca} -10$ to -15 kJ mol^{-1} . Our earlier estimate² that the amide-amide hydrogen bond between the acetyl carbonyl group of **1** and the NH of residue 7 contributes only $-2.9\pm 1.5 \text{ kJ mol}^{-1}$ to binding leads to the conclusion that the large apparent binding energies of the $-\text{CONH}_2$ group is attributable to more than just a hydrogen bonding interaction with the NH of residue 7. We have previously highlighted^{2,3} the comparison of the binding of N-Ac-Gly-D-Ala versus **1**, which, despite the removal of the hydrophobic contribution from an Ala methyl group (worth 53 \AA^2 of buried surface area), produces little net difference in binding energy between these two ligands (0.4 kJ mol^{-1} from calorimetry studies¹¹). Despite the loss of hydrophobic interactions, the Gly-ligand binds more exothermically to ristocetin by $\underline{ca} 6 \text{ kJ mol}^{-1}$. We propose that the removal of the Ala methyl group (Ala \rightarrow Gly) enables the *m*-dihydroxylated benzene ring of residue 7 of the antibiotic to approach more closely the π -face of the acetyl group of N-Ac-Gly-D-Ala, deriving some 6 kJ mol^{-1} additional exothermicity from this interaction (scheme D). The examination of molecular models strongly suggest that this is a real effect. Such exothermic π -

stacking interactions are known to occur from benzene-induced solvent shifts observed in the proton nmr spectrum of *N,N*-dimethylacetamide,¹³ which has long been rationalised in terms of weakly exothermic interactions of this type.



Such π -stacking interactions are also possible with ligands 2–5, but are precluded in 1 by the steric bulk of the N-terminal Ala methyl group. Thus, at least 6 kJ mol^{-1} of the apparent binding energy of the succinyl carboxyl group of 2 may be derived from this source. Our earlier conclusions³ that hydrogen bond strengths for neutral-neutral interactions typically lie in the range $-(0 \text{ to } 5) \text{ kJ mol}^{-1}$,¹⁴ together with values derived from protein engineering experiments $(-2 \text{ to } -8 \text{ kJ mol}^{-1})$,^{15,16} indicate that π -stacking contributions to the binding energy of the $-\text{CONH}_2$ group of 3 may realise somewhat more than 6 kJ mol^{-1} ($10 \pm 5 \text{ kJ mol}^{-1}$) of exothermicity from this interaction. To test our hypothesis that the carboxylate group of 2 must also bind with a large associated ΔH , we have estimated this parameter from van't Hoff plots of $\ln K$ versus $1/T$ for the binding of 2, for comparison with the available calorimetry data on 1. The average of five such plots leads to an estimate of ΔH for the binding of 2 in the range $-49 \pm 12 \text{ kJ mol}^{-1}$, considerably larger than the value of $-25.4 \pm 1.6 \text{ kJ mol}^{-1}$ measured for 1 by calorimetry.¹¹ Although there is some uncertainty in the former value, a large exothermic contribution (ca $-24 \pm 14 \text{ kJ mol}^{-1}$) to binding from the hydrogen bond and π -interactions with the carboxylate group of 2 seems inescapable. We note that charged hydrogen bonds have been shown experimentally to be stronger than neutral interactions (ca 12 kJ mol^{-1} versus $2 \text{ to } 8 \text{ kJ mol}^{-1}$),¹⁵ and thus substantial contributions to the carboxylate binding energy must be considered to arise from both hydrogen bonding and π -stacking.

Binding of oxamic acid derivatives 6 and 7.

The binding of 6 to ristocetin A benefits from the burial of some 29 \AA^2 more hydrocarbon surface than 7 ($\Delta\Delta G_h = -5.8 \pm 1.5 \text{ kJ mol}^{-1}$) but has the disadvantage of restricting at least 2, possibly as many as 3 additional alkyl chain rotors. The origin of the uncertainty in the number of rotors restricted (ΔN_r) lies in the effects of carboxylate-benzyl and amide-benzyl ring conjugation on the energy barriers to rotation about these bonds in 7, which may already be significantly restricted in the free ligand and suffer little further restriction in the bound state. We approximate ΔN_r as lying between 2 and 3, thus the difference in binding energy between 6 and 7 of $4.1 (\pm 1.5) \text{ kJ mol}^{-1}$ is partitioned as follows, using equation (2):

$$(4.1 \pm 1.5) = \Delta N_r \Delta G_r + (-5.8 \pm 1.5)$$

We conclude that the additional rotors restricted in the binding of 6 are contributing adversely to binding in the range $3.3 \text{ to } 5 \text{ kJ mol}^{-1}$ per rotor, in good agreement with our earlier assessment,^{7,12} and with the values derived and used in this paper ($2 \text{ to } 4 \text{ kJ mol}^{-1}$). Molecular modelling with both 6 and 7 indicate good ligand-receptor

complementarity in which hydrogen bonding interactions in the energy minimised structures are within the geometrical limits usually accepted for good interactions (close to linearity, O—N distance <3 Å), with the conformation of the bound ligands closely resembling the lowest energy conformations of the free ligands ($\Delta G_{\text{conf}} \approx 0$). On this basis we are led to the conclusion that the difference in binding energy is represented, to a useful approximation, by equation (2).

We similarly assess the binding contribution from the N-terminal carboxylate group of **6** and **7** by partitioning free energy contributions with respect to **1** and **8**, as described above for **2**. The natural substrate **1**, buries ca 108 Å² more non-polar surface area than **6**, but one fewer rotor is restricted at an extra cost ($\Delta\Delta G_r$) to **6** of (3±1) kJ mol⁻¹, $\Delta\Delta G$ being +11.1 (±0.9) kJ mol⁻¹. The amide-amide hydrogen bond of the acetyl group of **1** [worth -(2.9±1.5) kJ mol⁻¹],² is replaced by a carboxylate group whose contribution (ΔG_p) we now estimate from equation (2):

$$(11.1 \pm 0.9) = (3 \pm 1) + (22 \pm 5) + (2.9 \pm 1.5) + \Delta G_p$$

This gives ΔG_p as ca -17 (±8) kJ mol⁻¹. The same analysis with **6** versus **8** shows that the former buries ca 23 Å² less non-polar surface area at the additional cost of 3 extra rotors, despite the fact that the overall difference in binding energy is small [-0.3 (±1.0) kJ mol⁻¹ in favour of **6**]. The intrinsic binding energy of the carboxylate group is thus estimated:

$$-(0.3 \pm 1.0) = (9 \pm 3) + (5 \pm 1) + \Delta G_p$$

We deduce a ΔG_p value of ca -14 (±5) kJ mol⁻¹. The various contributions are summarised in Table 2.

The binding energy for the carboxylate interaction of **2** and **6**, deduced using four independent analyses, are remarkably consistent within the limitations and approximations of the methods employed, including errors in the experimental measurements. On the basis of our earlier conclusions regarding the strength of amide-amide hydrogen bonds [-(0 to 5) kJ mol⁻¹],³ and the results of others for charged interactions (up to ca 12 kJ mol⁻¹),¹⁵ we are led to the conclusion that a large component of the binding energy of the carboxylate interaction probed in these studies arises from face to face π - π stacking interactions. It has previously been shown by ¹³C NMR¹⁷ and convincingly by proton-proton NOE data¹⁸ that the benzene ring of residue 1 moves over the π -system of the carboxylate group of the natural substrate **1** in a manner exactly analogous to that proposed in the present study. Why might it do so? We conclude that the negative charge of the carboxylate is dispersed into the surrounding medium by the groups that hydrogen bond to it. Electron deficiency remains in the π -orbital of the carboxylate carbon; it is this charge that is likely to be energetically favourably solvated by the π -electron rich benzene ring of the antibiotic.

EXPERIMENTAL

General: All melting points are uncorrected and were obtained on a Kofler hot-stage apparatus. IR spectra were recorded on either a Perkin Elmer 1310 IR spectrometer or a Perkin Elmer 1600 FTIR spectrometer. Low and high resolution electron impact (EI) mass spectra were recorded on AEI MS902 and MS30 instruments, respectively. All solvents were distilled before use. Organic solutions were dried with anhydrous magnesium sulfate. Analytical tlc was carried out on 0.2 mm plates of Kieselgel F254 (Merck). Column chromatography was performed using Kieselgel 0.063-0.1 mm.

UV and NMR binding studies: UV spectra were recorded on a UVIKON 940 dual beam spectrometer at 298±2K. Antibiotic and ligand solutions were buffered with KH₂PO₄ (0.05 M)/NaOH (0.029 M), pH 7.0. Titrations were carried out using a two cell arrangement, as previously described.¹ All binding curves were measured in triplicate. Binding constants were derived from experimental data using Scatchard plots,¹ and the SIMPLEX least squares curve-fitting program.¹⁹

NMR Measurements: ¹H and ¹³C NMR spectra were recorded on a Bruker AM 400 spectrometer and were referenced to either tetramethylsilane or 3-trimethylsilylpropionic acid (d₄, sodium salt). For measurement of binding constants, sample concentrations of 0 to 10-100 mM of ligand were used with a constant concentration of antibiotic, with the solutions buffered as above. The chemical shift of protons in the ligand or on the binding face of the antibiotic were followed to indicate extent of binding. Binding constants were derived as for the UV data.

Synthesis—*N*-Succinyl-*D*-Alanine and *N*-fumaryl-*D*-Alanine were prepared as previously described.⁷

Mono-Methoxysuccinyl-*D*-alaninebenzylester: Mono-Methylsuccinic acid (227 mg, 1.72 mmol) and *D*-alaninebenzylester (600 mg, 1.73 mmol) were dissolved in dimethylformamide (10 mL). 4-Methylmorpholine (570 μL, 5.18 mmol) and 1-hydroxybenzotriazole (230 mg, 1.70 mmol) were added and the solution cooled to 0°C and 1-(3-dimethylaminopropyl)-3-ethylcarbodiimide hydrochloride (661 mg, 3.45 mmol) was added, and the reaction mixture stirred for 15 h at room temperature. Concentration at reduced pressure afforded a yellow oil that was taken up into water and repeatedly extracted into ethyl acetate. The organic extracts were combined, dried and concentrated to give 301mg (63%) of product as a white microcrystalline solid, m.p. 73-76°C. IR (NaCl) 3030, 1738 (br), 1656 cm⁻¹. ¹H NMR (CDCl₃) 1.38 (dd, J 7.2, 2.0 Hz, 3H, CH₃), 2.50, 2.63 (m, 4H, CH₂-CH₂), 3.64 (s, 3H, OCH₃), 4.61 (m, 1H, CH), 5.14 (m, 2H, OCH₂), 6.43 (br s, 1H, NH), 7.32 (m, 5H, Ar). ¹³C NMR 18.2 (CH₃), 29.0, 30.6 (CH₂-CH₂), 48.1 (OCH₃), 51.7 (CH), 67.0 (OCH₂), 128.3, 128.5, 128.6 (Ar), 135.2 (Ar), 170.9, 172.8, 173.2 (C=O). Anal. calcd. for C₁₅H₁₉NO₄, C, 61.50; H, 6.91; N, 5.05. Found C, 61.53; H, 6.66; N, 4.87.

***N*-Methylsuccinyl-*D*-alanine:** Mono-*N*-methylsuccinyl-*D*-alaninebenzylester (119 mg, 0.59 mmol) was dissolved in methanol (10 mL) and repeatedly degassed and flushed with argon. Palladium on charcoal (10%, 15 mg) was added and the reaction mixture was shaken under hydrogen (45 psi) for 18 h. Filtration and concentration at reduced pressure gave 82 mg (94%) of product as a white crystalline solid, m.p. 70-74°C. IR (NaCl) 3340, 2945 (br), 1740, 1720, 1640 cm⁻¹. ¹H NMR (CDCl₃) 2.10 (d, J 7.2Hz, 3H, CH₃), 2.55, 2.67 (m, 4H, CH₂-CH₂), 3.67 (s, 3H, OCH₃), 4.55 (m, 1H, CH), 6.66 (br d, 1H, NH), 6.89 (br s, 1H, OH). ¹³C NMR (CDCl₃) 17.9 (CH₃), 29.1, 30.6 (CH₂-CH₂), 48.2 (OCH₃), 52.0 (CH), 172.0, 173.5, 175.8 (C=O). Anal. calcd. for C₈H₁₃NO₄, C, 47.28; H, 6.45; N, 6.89. Found C, 46.57; H, 6.41; N, 6.80. *m/z* requires 203.1944. Found 203.1939.

***N*-Succinamyl-*D*-alanine:** *N*-Methylsuccinyl-*D*-alanine (48 mg, 0.26 mmol) was dissolved in water (2 mL) and cooled to 5°C. Concentrated aqueous ammonia (ca 14.8 M, 3 mL) was then added slowly and the reaction mixture stirred slowly at room temperature for 1 h. Concentration at reduced pressure afforded a residue that was taken up into water and reconstituted to give 40 mg (91%) of the product as a clear oil. IR (NaCl) 3300, 2980, 1725, 1680 cm⁻¹. ¹H NMR (D₂O) 1.38 (d, J 7.3Hz, 3H, CH₃), 2.62 (m, 4H, CH₂-CH₂), 4.19 (q, J 7.2Hz, 1H, CH). *m/z* C₇H₁₂N₂O₄ requires 188.1828. Found 188.1799.

***N*-Benzyloxycarbonyl-*D*-alaninemethoxyethoxymethyl ester:** *N*-Benzyloxycarbonyl-*D*-alanine (261 mg, 1.17

mmol) was dissolved in chloroform (10 mL) and *N,N*-diisopropylethylamine (510 μ L, 2.93 mmol) was added. The solution was cooled to 0°C and 2-methoxyethoxymethyl chloride (330 μ L, 2.89 mmol) was added dropwise. The reaction mixture was then stirred at room temperature for 90min, washed once with water, dried and concentrated to give a pale brown solid. Chromatography (1:1 ethyl acetate:hexanes) afforded 290 mg (83%) of the product as a clear oil. IR (NaCl) 2950, 1735, 1705 cm^{-1} . ^1H NMR (CDCl_3) 1.42 (d, J 7.2Hz, 3H, CH_3), 3.21 (s, 3H, OCH_3), 3.77 (m, 4H, $\text{OCH}_2\text{CH}_2\text{O}$), 3.88 (q, J 7.1Hz, 1H, CH), 5.10 (s, 2H, OCH_2O), 5.12 (s, 2H, CH_2Ar), 5.57 (br d, 1H, NH), 7.32 (m, 5H, Ar). *m/z* (%) $\text{C}_{14}\text{H}_{21}\text{NO}_6$ 299 [M^+] (100), 268 [M^+-OCH_3] (65).

D-Alaninemethoxyethoxymethyl ester: *N*-Benzyloxycarbonyl-*D*-alaninemethoxyethoxymethyl ester (105 mg, 0.35 mmol) was dissolved in methanol (8 mL) and repeatedly degassed and flushed with argon. Palladium on charcoal (5%, 15 mg) was added and the reaction mixture shaken under hydrogen (30 psi) for 15 h. Filtration and concentration gave 51 mg of the product (68%) as a white solid, m.p. 101-103 °C. IR (NaCl) 2970, 1740 cm^{-1} . ^1H NMR (CDCl_3) 1.50 (d, J 7.0Hz, 3H, CH_3), 3.22 (s, 3H, OCH_3), 3.81 (m, 4H, $\text{OCH}_2\text{CH}_2\text{O}$), 3.95 (q, J 7.1 Hz, 1H, CH), 5.05 (s, 2H, OCH_2O), 5.77 (br s, 2H, NH_2). *m/z* (%) $\text{C}_7\text{H}_{15}\text{NO}_4$ 177.1 [M^+] (95), 146 [M^+-OCH_3] (100).

N-Ethylfumaryl-D-alaninemethoxyethoxymethyl ester: Mono-ethylfumamic acid (70 mg, 0.49 mmol) and *D*-alaninemethoxyethoxymethyl ester (77 mg, 0.44 mmol) were dissolved in dimethylformamide (6 mL). 4-Methylmorpholine (150 μ L, 1.36 mmol) and 1-hydroxybenzotriazole (61 mg, 0.45 mmol) were added and the solution cooled to 0 °C. 1-(3-Dimethylaminopropyl)-3-ethyl-carbodiimide hydrochloride (175 mg, 0.91 mmol) was added and the reaction mixture stirred at room temperature for 16 h. Concentration afforded a yellow oil that was dissolved in water and repeatedly extracted into ethyl acetate. The organic extracts were combined, dried and the resulting solid purified by chromatography (1:2 ethyl acetate:hexanes) to give 61 mg (46%) of the product as a clear oil. IR (NaCl) 3040, 1750, 1725, 1670 cm^{-1} . ^1H NMR (CDCl_3) 1.32 (t, J 7.0Hz, 3H, CH_3CH_2), 1.43 (d, J 7.0 Hz, 3H, CH_3), 3.27 (s, 3H, OCH_3), 3.75 (m, 4H, $\text{OCH}_2\text{CH}_2\text{O}$), 4.31 (q, J 7.0Hz, 2H, CH_3CH_2), 4.60 (q, J 7.1 Hz, 1H, CH), 5.16 (s, 2H, OCH_2O), 6.88 (AB q, J 15.4 Hz, 2H, $\text{CH}=\text{CH}$), 6.61 (br d, J 5.7Hz, 1H, NH). *m/z* (%) $\text{C}_{13}\text{H}_{21}\text{NO}_7$ 303.2 [M^+] (60), 172.2 [M^+-OCH_3].

N-Ethylfumaryl-D-alanine: Ethylfumaryl-*D*-alaninemethoxyethoxymethyl ester (60 mg, 0.20 mmol) was dissolved in tetrahydrofuran (4 mL) and hydrochloric acid (2 M, 1 mL) was added. The reaction mixture was stirred at room temperature for 16 h, then concentrated and the residue dissolved in dichloromethane and washed successively with dilute aqueous sodium hydroxide, water, then dried and concentrated to afford 42 mg (98%) of the product as a pale yellow oil. IR (NaCl) 3015, 1725 cm^{-1} . ^1H NMR (CDCl_3) 1.31 (t, J 7.0 Hz, 3H, CH_3CH_2), 1.51 (d, J 6.9 Hz, 3H, CH_3), 4.26 (q, J 7.0 Hz, 2H, CH_3CH_2), 4.69 (q, J 6.4 Hz, 1H, CH), 6.95 (AB q, J 16.0 Hz, 2H, $\text{CH}=\text{CH}$), 7.42 (br d, J 5.9 Hz, 1H, NH), 9.73 (br s, 1H, COOH). ^{13}C NMR (CDCl_3) 13.9 (CH_3), 17.5 (CH_3CH_2), 48.7 (CH), 61.8 (CH_2O), 131.5, 135.5 ($\text{CH}_2=\text{CH}_2$), 164.6, 165.9, 175.9 (C=O). *m/z* (%) $\text{C}_9\text{H}_{13}\text{NO}_5$ 215.2 [M^+] (100).

N-Fumaramyl-D-alanine: *N*-Ethylfumaryl-*D*-alanine (111 mg, 0.56 mmol) was dissolved in water (4 mL) and cooled to 5 °C. Concentrated aqueous ammonia (ca 14.8 M, 4 mL) was added slowly and the reaction mixture stirred at room temperature for 1 h. Concentration then gave a residue that was dissolved in water and reconcentrated to afford 81 mg (78%) of the product as an off-white solid, m.p. 218-225 °C (dec.). IR (NaCl) 3260, 1710, 1645 cm^{-1} . ^1H NMR (D_2O) 2.26 (d, J 7.4Hz, 3H, CH_3), 5.11 (q, J 7.2 Hz, 1H, CH), 7.78 (AB q, J 16.0 Hz, 2H, $\text{CH}=\text{CH}$). *m/z* $\text{C}_7\text{H}_{10}\text{N}_2\text{O}_4$ requires 186.06405. Found 186.0637.

4-Aminobutanoic acid methylester: 4-Aminobutanoic acid (1 g, 9.7 mmol) was dissolved in methanol (30 mL) and thionyl chloride (1 mL, 13.7 mmol) was added dropwise with stirring. Concentration then afforded a residue that was washed with dichloromethane to give 850 mg (75%) of the product as a white crystalline solid, m.p. 97-101 °C. IR (NaCl) 2890, 1740 cm^{-1} . ^1H NMR (CD_3OD) 1.98 (p, J 7.4 Hz, 2H, $\text{CH}_2\text{CH}_2\text{CH}_2$), 2.51 (t, J 7.2 Hz, 2H, CH_2O), 3.02 (t, J 7.4 Hz, 2H, CH_2N), 3.69 (s, 3H, OCH_3), 4.83 (br s, 2H, NH_2). ^{13}C NMR (CD_3OD) 23.7 ($\text{CH}_2\text{CH}_2\text{CH}_2$), 31.5 (CH_2CO), 40.2 (CH_2N), 52.3 (CH_3O), 174.6 ($\text{C}=\text{O}$). m/z $\text{C}_5\text{H}_{11}\text{NO}_2$ requires 117.0680, found 117.0784.

N-Oxalyl-4-aminobutanoic acid dimethylester: 4-Aminobutanoic acid methyl ester hydrochloride (607 mg, 5.19 mmol) and 4-methylmorpholine (800 μL , 11.2 mmol) were dissolved in dichloromethane (30 mL). Methyloxalyl chloride (500 μL , 5.8 mmol) was added dropwise and the reaction mixture stirred at room temperature for 5 h. Successive washing with citric acid (10%, aqueous), sodium bicarbonate (saturated, aqueous) and water, then drying and concentration gave 451 mg (56%) of product as a clear oil. IR (NaCl) 3346, 1738, 1693, 1681 cm^{-1} . ^1H NMR (CDCl_3) 1.92 (p, J 7.0 Hz, 2H, $\text{CH}_2\text{CH}_2\text{CH}_2$), 2.40 (t, J 7.1 Hz, 2H, CH_2CO), 3.41 (q, J 6.6 Hz, 2H, CH_2N), 3.69 (s, 3H, OCH_3), 3.90 (s, 3H, OCH_3), 7.30 (br s, 1H, NH). m/z (%) 203.1 [M^+] (15), 144.1 [$\text{M}^+ - \text{CH}_2\text{CO}_2$] (55).

N-Oxalyl-4-aminobutanoic acid: N-Oxalyl-4-aminobutanoic acid dimethylester (451 mg, 2.58 mmol) was dissolved in an aqueous solution of lithium hydroxide (ca 1 M) and stirred at room temperature for 16 h. Treatment with Dowex-50 (protonated form) and concentration gave 389 mg (80%) of the product as a white microcrystalline solid, m.p. 155-159 °C. IR (NaCl) 3420 (br), 1720, 1624 cm^{-1} . ^1H NMR (D_2O) 1.87 (p, J 7.0 Hz, 2H, $\text{CH}_2\text{CH}_2\text{CH}_2$), 2.44 (t, J 7.3 Hz, 2H, CH_2CO), 3.33 (t, J 6.8 Hz, 2H, CH_2N). m/z (%) 175.1 [M^+] (1), 130.1 [$\text{M}^+ - \text{CO}_2\text{H}$] (30).

3-Aminobenzoic acid methylester: 3-Aminobenzoic acid (2.01 g, 14.6 mmol) was dissolved in methanol (30 mL) and thionyl chloride (1.5 mL, 15.9 mmol) was added dropwise with stirring. Concentration then afforded a residue that was washed with dichloromethane to give 2.19 g (79%) of the product as a white microcrystalline solid, m.p. 148-152 °C. IR (NaCl) 3410, 1653 cm^{-1} . ^1H NMR (CD_3OD) 3.95 (s, 3H, CH_3), 7.70 (m, 2H, ArH), 8.10 (s, 1H, ArH), 8.12 (m, 1H, ArH). ^{13}C NMR (CD_3OD) 53.1 (CH_3O), 125.2, 128.9, 131.0, 131.7, 132.5, 133.4 (Ar), 166.8 ($\text{C}=\text{O}$). Anal. calculated for $\text{C}_8\text{H}_{10}\text{ClNO}_2$: C, 51.21; H, 5.37; N, 7.47. Found C, 51.11; H, 5.35; N, 7.43.

N-Oxalyl-3-aminobenzoic acid methylester: 3-Aminobenzoic acid methyl ester (966 mg, 5.12 mmol) and 4-methylmorpholine (1.15 mL, 10.4 mmol) were dissolved in dichloromethane (25 mL). Methyloxalyl chloride (500 μL , 5.5 mmol) was then added dropwise, and the reaction mixture stirred at room temperature for 5 h. Successive washing with citric acid (10%, aqueous), sodium bicarbonate (saturated, aqueous) and water, then drying and concentration gave 820 mg (87%) of product as a white microcrystalline solid, m.p. 160-163 °C. IR (NaCl) 3425, 1702, 1646 cm^{-1} . ^1H NMR (CDCl_3) 3.93 (s, 3H, OCH_3), 3.98 (s, 3H, OCH_3), 7.47 (t, J 8.0 Hz, 1H, ArH), 7.87 (d, J 7.8 Hz, 1H, ArH), 8.01 (dd, J 8.0, 1.6 Hz, 1H, ArH), 8.14, (d, J 1.6 Hz, 1H, ArH), 8.95 (br s, 1H, NH). ^{13}C NMR (CDCl_3) 52.3 (OCH_3), 54.1 (OCH_3), 120.8, 124.2, 126.6, 129.5, 131.3, 136.5 (Ar), 153.8, 161.2, 166.3 ($\text{C}=\text{O}$). m/z (%) 237.2 [M^+] (45), 178.2 [$\text{M}^+ - \text{CH}_2\text{CO}_2$] (100).

N-Oxalyl-3-aminobenzoic acid: N-Oxalyl-3-aminobenzoic acid methylester (715 mg, 3.0 mmol) was dissolved in an aqueous solution of lithium hydroxide (ca 1 M) and stirred at room temperature for 18 h. Treatment with Dowex-50 (protonated form) and concentration gave 530 mg (85%) of the product as a white powder, m.p. 256-261 °C. IR (NaCl) 3420, 1686, 1637 cm^{-1} . ^1H NMR (D_2O) 7.52 (t, J 7.9 Hz, 1H, ArH), 7.76 (d, J 7.9 Hz,

1H, ArH), 7.78 (d, J 7.9 Hz, 1H, ArH), 8.04 (s, 1H, ArH). *m/z* C₉H₇NO₅ requires 209.03242, found 209.0315.

Acknowledgements

We thank the SERC (UK), the Upjohn Company (Kalamazoo) and Lilly Research Laboratories (UK) for financial support. UG thanks BASF for a Churchill College studentship; PG thanks Xenova and SERC for a CASE studentship.

References and Notes

1. Williams, D. H.; Cox, J. P. L.; Doig, A. J.; Gardner, M.; Gerhard, U.; Kaye, P. T.; Lal, A. R.; Nicholls, I. A.; Salter, C. J.; Mitchell, R. C., *J. Am. Chem. Soc.* **1991**, *113*, 7020-7030.
2. Searle, M. S.; Williams, D. H.; Gerhard, U., *J. Am. Chem. Soc.* **1992**, *114*, 10697-10704.
3. Williams, D. H.; Searle, M. S.; Mackay, J. P.; Gerhard, U.; Maplestone, R. A., *Proc. Natl. Acad. Sci. USA* **1993**, *90*, 1172-1178.
4. Jencks, W. P., *Proc. Natl. Acad. Sci. USA* **1981**, *78*, 4046-4050.
5. Page, M. I.; Jencks, W. P., *Proc. Natl. Acad. Sci. USA* **1971**, *68*, 1678-1683.
6. The adverse free energy (mainly entropy) of a bimolecular association (ΔG_{T+R}) should be essentially the same for ligands of similar mass (since ΔG_{T+R} depends only on the logarithm of the mass) if they also bind with similar exothermic barriers to dissociation.³
7. Gerhard, U.; Searle, M. S.; Williams, D. H., *Bio-org. Med. Chem. Lett.* **1993**, in press.
8. Williams, D. H.; Kalman, J. R., *J. Am. Chem. Soc.* **1977**, *99*, 2768-2774.
9. Mohamadi, F.; Richards, N. G. J.; Guida, W. C.; Liskamp, R.; Lipton, M.; Caufield, C.; Chang, G.; Hendrickson, T.; Still, W. C., *J. Compt. Chem.* **1990**, *11*, 440-467.
10. Serrano, L.; Neira, J.-L.; Sancho, J.; Fersht, A. R., *Nature* **1992**, *356*, 453-455.
11. Rodriguez-Tebar, A.; Vazquez, D.; Perez Velazquez, J. L.; Laynez, J.; Wadso, I., *J. Antibiot.* **1986**, *39*, 1578-1583.
12. Searle, M. S.; Williams, D. H., *J. Am. Chem. Soc.* **1992**, *114*, 10690-10697.
13. Hatton, J. V.; Richards, R. E., *Mol. Phys.* **1962**, *5*, 139-144.
14. Conclusions from seven out of nine data sets considered in reference 2, but excluding the values of -7 and -12 kJ mol⁻¹ derived from glycine extensions which are concluded to be associated with the same additional exothermic π -stacking interaction.
15. Fersht, A. R., *Trends Biochem. Sci.* **1987**, *12*, 301-304.
16. Shirley, B. A.; Stanssens, P.; Hahn, U.; Pace, C. M., *Biochemistry* **1992**, *31*, 725-732.
17. Williamson, M. P.; Williams, D. H., *J. Chem. Soc. Perkin I* **1981**, 1483-1490.
18. Waltho, J. P.; Williams, D. H., *J. Am. Chem. Soc.* **1989**, *111*, 2475-2480.
19. Press, W. H.; Flannery, B. P.; Tenkolsky, S. A.; Vetterling, W. T., *Numerical Recipes in Pascal*, **1989**, Cambridge University Press.